JOURNAL OF PHYSICAL ORGANIC CHEMISTRY
J. Phys. Org. Chem. 2007; **20:** 271–284
Published online 29 March 2007 in Wiley InterScience
(www.interscience.wiley.com) DOI: 10.1002/poc.1164

Investigation of *N*-carbamoylamino acid nitrosation by {NO + O_2} in the solid-gas phase. Effects of NO_x speciation and kinetic evidence for a multiple-stage process

Olivier Lagrille, Jacques Taillades, Laurent Boiteau* and Auguste Commeyras

Dynamique des Systèmes Biomoléculaires Complexes, UMR CNRS 5247, Chemistry Department, University of Montpellier 2, Place Eugène Bataillon, F-34095 Montpellier Cedex 5, France

Received 14 September 2006; revised 23 November 2006; accepted 12 December 2006

ABSTRACT: Nitrosation of *N*-carbamoylamino acids (CAA) by gaseous NO + O_2, an interesting synthetic pathway to amino acid *N*-carboxyanhydrides (NCA), alternative to the phosgene route, was investigated on *N*-carbamoyl-valine either in acetonitrile suspension or solventless conditions, and compared to the classical nitrosating system $NaNO_2$ + CF_3COOH (TFA), the latter being quite less efficient in terms of either rate, stoichiometric demand, or further tractability of the product. The rate and efficiency of the NO + O_2 reaction mainly depends on the O_2/NO ratio. Evaluation of the contribution of various nitrosating species (N_2O_3, N_2O_4, HNO_2) through stoichiometric balance showed the reaction to be effected mostly by N_2O_3 for O_2/NO ratios below 0.3, and by N_2O_4 for O_2/NO ratios above 0.4. The relative contribution of (subsequently formed) HNO_2 always remains minor. Differential scanning calorimetry (DSC) monitoring of the reaction in the solid phase by either HNO_2 (from $NaNO_2$ + TFA), gaseous N_2O_4 or gaseous N_2O_3, provides the associated rate constants (ca. 0.1, 2 and 10^8 s^{-1} at 25°C, respectively), showing that N_2O_3 is by far the most reactive of these nitrosating species. From the DSC measurement, the latent heat of fusion of N_2O_3, 2.74 kJ · mol^{-1} at −105 °C is also obtained for the first time. The kinetics was investigated under solventless conditions at 0°C, by either quenching experiments or less tedious, rough calorimetric techniques. Auto-accelerated, parabolic-shaped kinetics was observed in the first half of the reaction course, together with substantial heat release (temperature increase of ca. 20°C within 1–2 min in a 20-mg sample), followed by pseudo-zero-order kinetics after a sudden, important decrease in apparent rate. This kinetic break is possibly due to the transition between the initial solid-gas system and a solid-liquid-gas system resulting from water formation. Overall rate constants increased with parameters such as the specific surface of the solid, the O_2/NO ratio, or the presence of moisture (or equivalently the hydrophilicity of the involved CAA), however without precise relationship, while the last two parameters may directly correlate to the increasing acidity of the medium. Copyright © 2007 John Wiley & Sons, Ltd.
Supplementary electronic material for this paper is available in Wiley Interscience at http://www.interscience.wiley.com/jpages/0894-3230/suppmat/.

KEYWORDS: amino acid N-carboxyanhydrides; nitrosation; N-carbamoylamino acids; kinetics; solid-phase reaction

INTRODUCTION

The synthesis of amino acid *N*-carboxyanhydrides (NCA, also known as Leuchs anhydrides) **1** is subject to important research efforts, due to their interest as key monomers in the synthesis of polypeptide materials. Classical synthetic routes to NCA usually involving Leuchs[1] or Fuchs–Farthing[2,3] methods (Scheme 1), present major drawbacks such as the toxicity of involved reagents (e.g. phosgene), or the difficulty of separating side-products, in spite of important efforts made to improve them by the use of either more efficient leaving groups, or reagents less toxic than phosgene.[4,5]

Our previous work dealing with the relevance of *N*-carbamoylamino acids (CAA) **2** as possible prebiotic precursors of peptides,[6] led us to examine CAA activation pathways and to discover that their nitrosation by a NO + O_2 gaseous mixture resulted into smooth, fast NCA formation (Scheme 2) with nitrogen and water as the only side products.[7] NMR monitoring (in DMSO-d_6) showed

**Correspondence to:* Dr L. Boiteau, DSBC (UMR5247)-CC.017, University Montpellier-2, Place Eugene Bataillon, F-34095 Montpellier Cedex 5, France.
E-mail: laurent.boiteau@univ-montp2.fr

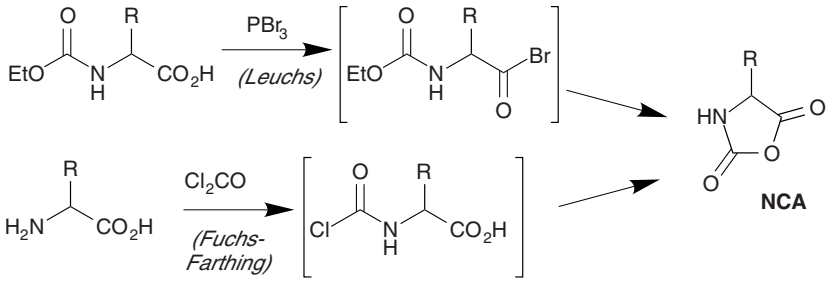

Scheme 1

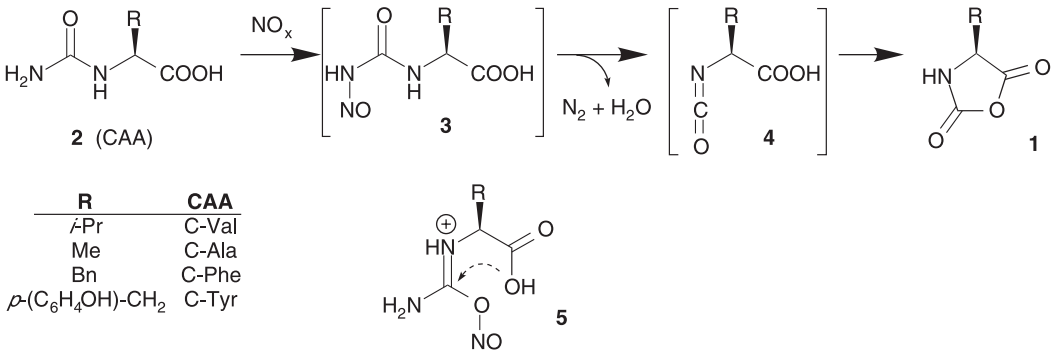

Scheme 2

the reaction to proceed through the fast formation of an intermediate (assumed to be an external *N*-nitrosourea **3**), followed by its slower decomposition into nitrogen, water and NCA, most likely through a transient isocyanate intermediate **4**.[7] The early intermediacy of an amidium-type species **5** resulting from the *O*-nitrosation of urea, is very probable.[8,9] However a further addition-elimination mechanism on **5** involving the vicinal carboxy group is likely disfavoured according to Baldwin's rules[10,11] since it would involve a *5-endo-trig* cyclisation, so that its rearrangement into **3** is more plausible. Such addition-elimination pathway (involving either **3** or **5**) may occur as an alternative to isocyanate formation when the latter is impossible, for example from *N*,*N*-dialkyl ureas.[12] Nevertheless such mechanistic issues are not the focus of the present paper and will be discussed in a future publication.

One of the major features of CAA nitrosation is that it occurs in the heterogeneous phase since CAAs are insoluble in most organic solvents, including acetonitrile used in previous investigations. This led us to investigate the reaction without solvent, meanwhile the prebiotic relevance of such a pathway was also discussed.[13] This new synthetic route to NCA opened new application perspectives as a potent eco-friendly challenger to phosgene routes, thus pointing to the need for further investigations.

Reaction in the solid phase. Although probably proceeding according to the same pathway, the reaction in the solid phase appears somewhat more complex. Monitoring the $NO + O_2$-mediated nitrosation of *N*-carbamoyl valine, C-Val, crystals by optical microscopy showed the reaction not to proceed in a truly solid phase: the solid surface readily wets, while gas bubbles evolve. While the reaction actually starts as a solid-gas process, the water released together with NCA formation partly dissolves the solid material and NO_x species, thus allowing the reaction to progress also in the liquid phase. At the end of the reaction however, the crude product is often recovered as a solid and not as an oil: nitrogen evolution and exothermicity of the reaction probably contribute to evaporate the water as and when it is formed.

Previous investigation of solid-gas nitrosation of C-Val in a fluid-bed reactor by various NO/O_2 stoichiometries with monitoring the total NO_x consumption showed zero-order kinetics,[13] however without allowing to investigate other reaction parameters. Furthermore, those experiments were poorly reproducible especially regarding the final CAA-to-NCA conversion. Further investigation was then necessary to better understand the reaction in view of future synthetic applications.

In this paper, we present deeper insights in the efficiency and kinetics of solventless CAA nitrosation by $NO + O_2$, investigating valine as the model amino acid, with comparison to the reaction in acetonitrile suspension, and to the more classical nitrosating system {nitrite + trifluoroacetic acid (TFA)}, the latter being considered as the reference for further evaluation of $\{NO + O_2\}$ efficiency. NO_x speciation (O_2/NO ratio) is chiefly concerned since several species coexist in

DOI: 10.1002/poc

$\{NO + O_2\}$ mixtures, those of major interest here being N_2O_3 and N_2O_4 (both of them are formally NO^+ donors[14]). Since water is generated during NCA formation, we also consider the nitrosating species HNO_2 separately generated from the system {nitrite + TFA}.

RESULTS AND DISCUSSION

N-carbamoyl valine C-Val was prepared according to our previously published procedures,[15] by reaction of the free amino acid with aqueous potassium cyanate, under pH regulation to 7–8, then easily purified by recrystallisation from water. NO_x nitrosating mixtures were obtained in all cases by mixing appropriate amounts of NO and O_2 at atmospheric pressure, usually in stoichiometric excess compared to CAA so that the pressure and stoichiometric composition of the equilibrated NO_x mixture should not significantly vary along the reaction progress.

Nitrosation of C-Val by nitrite + TFA in acetonitrile (the reference system)

We investigated HNO_2-mediated nitrosation of C-Val by using the conventional system {sodium nitrite + trifluoroacetic acid} in acetonitrile (Table 1). The use of moderate excess of nitrite and acid gives good conversion (evaluated by integration of the Hα peaks on NMR spectra) within 2 h. To estimate the relative rate of this system compared to that of the $NO + O_2$ system, the conversion was measured after 5 min, evaluating the remaining C-Val by HPLC analysis after quenching the reaction by an excess of sodium hydroxide. While the reaction is significantly retarded by any excess of nitrite over TFA, the catalytic effect of TFA is obvious, in particular when in excess over nitrite, which suggests the involvement of the acidic form. The origin of such catalysis can be either general acid catalysis with formation of the faster nitrosating species NO^+ (Eqn 1), or the formation of nitrosyl trifluoroacetate CF_3CO_2NO as an intermediate (Eqn 2). This species has been reported as an efficient nitrosyl-transferring agent,[16] as well as other nitrosyl carboxylates, for example acetate.[17–19]

$$NO_2^- \overset{CF_3CO_2H}{\rightleftharpoons} HNO_2 \overset{CF_3CO_2H}{\rightleftharpoons} H_2NO_2^+ \rightleftharpoons NO^+ + H_2O \quad (1)$$

$$CF_3CO_2H + HNO_2 \leftrightharpoons CF_3CO_2NO + H_2O \quad (2)$$

It deserves to note that, although efficient and easy to carry out, the nitrosation of CAA by the {TFA + nitrite} system offers poor perspectives in a NCA preparative scope compared to the $\{NO + O_2\}$ method, since the presence of salts and water in the reaction mixtures makes the further purification of NCA very difficult.

Nitrosation of C-Val by $NO + O_2$

Gaseous mixtures of NO and O_2 react at room temperature, readily forming rather complex mixtures of O_2, NO, NO_2, N_2O_3, N_2O_4,[14] the two latter species being responsible for the nitrosation reaction. Equilibrium stoichiometry of such $\{NO + O_2\}$ mixtures is mainly governed by Eqns 3–5 (equilibrium constants at 25°C were evaluated from standard formation enthalpies

Table 1. Nitrosation of C-Val (100 mg) by $NaNO_2$ + TFA (various amounts) in acetonitrile (50 ml) at room temperature: effect of reagent stoichiometry (NCA yield not measured when quenched after 5 min reaction)

		Initial conditions			Working conditions				
Run	Time/min	$[NO_2^-]/[CAA]$	$[TFA]/[NO_2^-]$	$[TFA]/[CAA]$	$[NO_2^-]/[CAA]$	$[HNO_2]/[CAA]$	$[NO^+]/[CAA]$	Conv. %	NCA yield %
1	30	1.5	1	1.5	0	1.5	0	95	71
2	120	1.5	1.33	2	0	1	0.5	71	63
3	120	1	2	2	0	0	1	87	79
4	5	12	0.25	3	9	3	0	15	n.m.
5	5	6	0.5	3	3	3	0	44	n.m.
6	5	3	1	3	0	3	0	58	n.m.
7	5	3	2	6	0	0	3	100	n.m.
8	5	1	1	1	0	1	0	11	n.m.
9	5	2	0.5	1	1	1	0	16	n.m.
10	5	4	0.25	1	3	1	0	5	n.m.
11	5	1	2	2	0	1	0	38.5	n.m.
12	5	1.5	1	1.5	0	1.5	0	31	n.m.
13	5	0.75	1	0.75	0	0.75	0	12.5	n.m.

Working conditions: equilibrated TFA-nitrite mixture according to Eqns 1–2 considered as completely shifted to the right.

DOI: 10.1002/poc

ΔH_f^0 and entropies ΔS_f^0 of the involved species[20–22]):

$$NO_2 \leftrightarrows NO + 1/2O_2 \quad (K_1 = 2.77 \times 10^{-12}\,\text{atm}^{1/2}, 25°C) \tag{3}$$

$$N_2O_3 \leftrightarrows NO + NO_2 \quad (K_2 = 2.12\ \text{atm},\ 25°C) \tag{4}$$

$$N_2O_4 \leftrightarrows 2NO_2 \quad (K_3 = 0.148\ \text{atm},\ 25°C) \tag{5}$$

Due to the very low K_1 (Eqn 3 completely shifted to the left), if $O_2/NO > 0.5$ the species NO and N_2O_3 are almost absent from equilibrated mixtures, with pressures of both NO_2 and N_2O_4 independent of the O_2/NO ratio. Conversely, if $O_2/NO < 0.5$, the amount of N_2O_4 increases almost linearly with the O_2/NO ratio, while N_2O_3 remains a minor component (at most a few mol% around $O_2/NO = 0.25$). This occurs over a wide range of NO initial pressures.

The nitrosation of C-Val by $\{NO + O_2\}$ was examined in both acetonitrile suspension and solid-gas phase (without solvent). The evolution of the (exothermic) reaction could be easily followed by the rapid discolourisation of the gaseous phase. In all cases, the reaction was complete within ca. 10–30 min. Meanwhile a lagoon-blue colour (characteristic of condensed N_2O_3 and N_2O_4) transiently appeared in the condensed phase, together with heat release.

In the organic suspension, the insoluble, solid CAA progressively disappeared and was converted into soluble NCA. In the solid phase, water droplets condensed onto the walls of the flask. Previous optical microscopy monitoring showed that a liquid phase forms onto the solid material, together with gas bubble evolution. However, in most cases the final product was recovered as a solid.

The conversion appears mainly dependent on the CAA/NO/O_2 stoichiometry (Figure 1). No reaction occurs in the absence of oxygen. With a starting stoichiometry NO/CAA = 1, the conversion increases upon increasing the O_2/NO ratio up to ca. 60% at $O_2/NO = 0.2$–0.3, roughly corresponding to the N_2O_3 overall stoichiometry, then decreases to ca. 40%. When higher NO/CAA stoichiometries are used, the same trend is observed (in acetonitrile) with higher conversion, up to 100%; the minimum O_2/NO/CAA stoichiometry required for a quantitative conversion is 0.6/2/1 and again, the reaction efficiency decreases with increasing O_2/NO ratios. It is intriguing to observe a so small difference between acetonitrile and solventless conditions: Bravo *et al.*[23] observed significant solvent effects in various acetonitrile/water mixtures, with mechanistic change with the water/acetonitrile ratio and higher rates in pure solvents than in mixtures. However, our solventless conditions may not be properly described by a dilute aqueous solution. Retarding effects have also been observed in acetonitrile at a lower temperature (−40°C) by Darbeau *et al.*,[9] who suspected acetonitrile to behave as a NO^+ transfer agent in spite of the supposed inertness of the nitrile group.

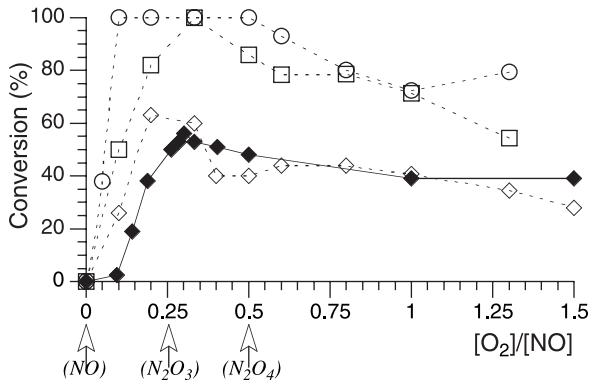

Figure 1. Nitrosation of C-Val by $NO + O_2$ at room temperature and atmospheric pressure: conversion after 30 min reaction as a function of the O_2/NO stoichiometric ratio. Reactions carried out in acetonitrile with 625 μmol C-Val (open symbols) or in the solid-gas phase with 187.5 μmol (filled symbols) with NO/C-Val stoichiometric ratios of 1 (diamonds), 2 (squares) or 3 (circles). Experimental points are connected visually for an easy reading

Involved nitrosating species and their relative efficiency (NO_x speciation)

CAA nitrosation involving either N_2O_3 or N_2O_4 (Eqns 6–7), as well as N_2O_3/N_2O_4 hydrolysis (by water subsequently released together with NCA formation, Scheme 2) releases nitrous and/or nitric acid, respectively. The resulting acidification of the medium (certainly very strong under 'dry phase' conditions where reactive species are highly concentrated in the condensed phase) allows HNO_2-mediated nitrosation to take place through the protonated, very reactive species $H_2NO_2^+$[24] (as with the {nitrite + TFA} system), a pathway much faster than the slow dehydration of HNO_2 into N_2O_3.[25]

$$\mathbf{CAA} + N_2O_3 \rightarrow \mathbf{3} + H^+ + NO_2^- \tag{6}$$

$$\mathbf{CAA} + N_2O_4 \rightarrow \mathbf{3} + H^+ + NO_3^- \tag{7}$$

$$\mathbf{CAA} + H_2NO_2^+ \rightarrow \mathbf{3} + H_3O^+ \tag{8}$$

Measurement of nitrite and nitrate anions in crude reaction mixtures (by capillary electrophoresis after alkaline quenching) therefore leads to the evaluation of the relative contributions of N_2O_3, N_2O_4 and HNO_2 to the overall nitrosation process – N_2O_4 being quantitatively related to nitrate (Eqn 7), N_2O_3 to nitrite (Eqn 6) after correction of the overall imbalance corresponding to $HNO_2/H_2NO_2^+$ consumption (Eqn 8, the latter pathway releasing no anion). Direct hydrolysis of N_2O_3/N_2O_4 turned out to be negligible (not exceeding a few per cent in blank experiments). We also assumed the dismutation of HNO_2 into NO, H_2O and HNO_3 (usually occurring at high temperatures) to be sufficiently slow under our conditions to be negligible as well.[14] What could not be

DOI: 10.1002/poc

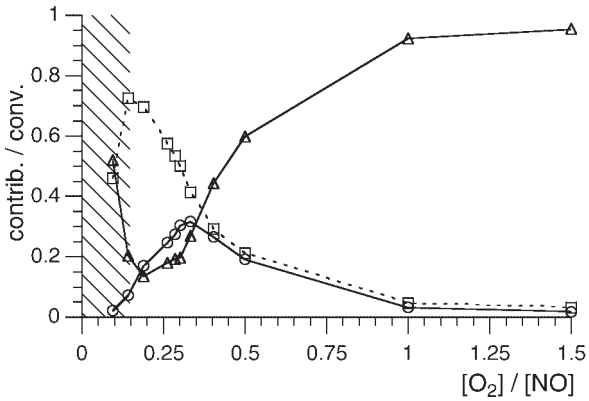

Figure 2. Contribution of the different nitrosating species in dry nitrosation of solid C-Val by {NO + O_2} at room temperature, compared to overall conversion, as a function of O_2/NO ratio: N_2O_3 (squares), HNO_2 (circles) and N_2O_4 (triangles). Hashed area: unreliable results because of uncertainty in the (measured) low conversion range (<10%)

neglected is the formation of additional nitrite anions from dismutation of unreacted NO during alkaline quenching, a phenomenon occurring for O_2/NO ratios below 0.5 and inducing up to 25% bias in nitrite measurement. Quantification of the phenomenon on blank experiments allowed correcting it satisfactorily.

Results of the relative contribution of NO_x species to overall conversion versus O_2/NO ratios are shown in Figure 2. Relative contributions of N_2O_3 and N_2O_4 do not follow their equilibrium ratio in the gas phase, meaning that equilibria Eqns 1–3 are actually shifted during the nitrosation reaction. N_2O_4 is the major contributor with O_2/NO ratios larger than 0.4, while N_2O_3 is the major contributor when O_2/NO ratios are smaller than 0.3. The apparent trend inversion observed at the lowest O_2/NO ratios (<0.15) is questionable because of the inaccuracy of measured low conversion values and would require further investigation. In all cases HNO_2 ($H_2NO_2^+$) contributes to a smaller extent to the overall process, its contribution appearing roughly as the intersection of the N_2O_3 and N_2O_4 curves. This suggests that a stoichiometric amount of either N_2O_4 or HNO_3 would be required to ensure HNO_2^+-mediated nitrosation from HNO_2, while catalytic amounts were expected to be sufficient since protons are supposedly regenerated after the nitrosation step (Eqn 8). Possible reasons can be kinetic, with for instance the slow decay of subsequent cationic intermediates.

Thermoanalytical kinetic investigation

Thermochemical and kinetic parameters of the nitrosation reaction involving either N_2O_4, N_2O_3 or HNO_2/NO^+ without solvent, were investigated through differential scanning calorimetry (DSC) monitoring, a technique allowing to measure both the reaction heat ΔH^r, as well as its apparent rate constant k and activation energy E_A. ΔH is directly given by DSC peak integration. Assuming that the reaction is pseudo first-order ($[-d\xi/dt = k(T) \cdot \xi]$ with ξ, the reaction extent) and follows the Arrhenius law $[k(T) = A \cdot \exp(-E_A/RT)]$, parameters E_A and A were determined by fitting of simulated thermograms (easily computed from given ΔH, E_a and A at various temperature scanning rates) to experimental ones.

Nitrosation by HNO_2/NO^+ (the reference system) was investigated through the {$NaNO_2$ + TFA} system, with TFA/nitrite stoichiometric ratios of 1/1, 2/1 and 10/3 (the nitrite/C-Val stoichiometric ratio was 3/1 in all cases). DSC curves exhibit first a small endotherm (TFA melting), then two exotherms corresponding to TFA-nitrite neutralisation and to C-Val nitrosation, respectively. An increase in TFA/nitrite ratios resulted into sharper nitrosation peaks, meaning a significant increase in the reaction rate.

Measured thermochemical and kinetic data are shown in Table 2. The obtained reaction heat (ΔH) for a TFA/nitrite ratio of 1/1 ($-136\,kJ\ mol^{-1}$), far below those measured for TFA/nitrite ratios of 2/1 and 10/3 ($-230\,kJ\ mol^{-1}$), suggests the reaction to be incomplete in the first case (ca. 60% extent), as observed in acetonitrile suspension, thus questionning the reliability of associated kinetic parameters. The substantial increase

Table 2. DSC data for nitrosation of C-Val (12.5 μmol) by sodium nitrite (3 eq.) + TFA (3, 6, 10 eq.): reaction enthalpy ΔH (average of several measurements), DSC peak temperature T_m; calculated 1st-order kinetic parameters (activation energy E_A, pre-exponential factor A, extrapolated rate constant k at 25°C)

[TFA]/[NO_2^-]	**1** (3/3)		**2** (6/3)		**3.33** (10/3)	
DSC rate/°C min^{-1}	**5**	**8**	**5**	**8**	**5**	**8**
$-\Delta H$ ($kJ \cdot mol^{-1}$)	134.1	138.9	228.6	232.4	228.5	231.8
Average	−136.5		−230.5		−230.2	
T_m (°C)	−1.7	−2.0	1.9	3.1	0.0	3.0
E_A ($kJ \cdot mol^{-1}$)	104.5	96.1	107.4	97.7	193.1	185.6
Average	100		103		189	
A (s^{-1})	1.5×10^{18}	5.1×10^{17}	2.8×10^{18}	1.9×10^{16}	1.5×10^{35}	1.1×10^{34}
Average	$1.0(\pm 0.5) \times 10^{18}$		$2.8(\pm 0.02) \times 10^{18}$		$0.8(\pm 0.7) \times 10^{35}$	
$k_{25°C}$ (s^{-1})	$7.0(\pm 0.4) \times 10^{-1}$		$3.6(\pm 0.4) \times 10^{-1}$		$2.4(\pm 0.6) \times 10^{1}$	

DOI: 10.1002/poc

in the rate constant with TFA/nitrite ratio strongly suggests a catalytic effect of TFA, either due to general acid catalysis (responsible for the faster formation of NO^+ intermediates), or due to the involvement of trifluoroacetyl nitrite as an intermediate.[26] From our calculated kinetic parameters, the rate constant extrapolated to 25°C is around 0.1 s^{-1} (k_{HNO_2}).

Nitrosation by (gaseous) N_2O_3 or N_2O_4 was investigated on C-Val in the solid-gas phase. In this purpose, a small PTFE (Teflon) cup containing solid C-Val was placed inside the DSC crucible containing the frozen NO_x, to avoid premature contact between the reacting species. All reactions were carried out with an excess of nitrosating reagent. N_2O_3 was prepared according to the well-known procedure involving nitric acid reduction by As_2O_3 just prior to DSC experiments.[27]

In blank experiments without C-Val, melting endotherms occurring at −105°C (N_2O_3) or −13.2°C (N_2O_4), allowed to determine the latent melting heat of these species, 2.74 and 16.77 kJ · mol^{-1}, respectively. While our measurement for N_2O_4 is in good agreement with previously published data (14.65 kJ · mol^{-1} at N_2O_4 triple point[28]), this is the first report of an experimental value of N_2O_3 melting heat. With both N_2O_3 and N_2O_4 the nitrosation exotherm observed far below the boiling point of the NO_x species (ca. +3°C and +21°C for N_2O_3 and N_2O_4, respectively), confirms that the nitrosation was effected by gaseous NO_x at saturating vapour pressure. Thermogramms involving N_2O_4 were processed after subtraction of N_2O_4 phase-transition endotherms (DSC curves of blanks) otherwise interfering with the nitrosation reaction. Conversely to the {TFA + nitrite} case, the use of various stoichiometric excesses of N_2O_3 and N_2O_4, resulted in only small changes in thermochemical and kinetic results (Table 3). Measurements of reaction enthalpies for C-Val nitrosation involving both N_2O_3 and N_2O_4, (Table 3) appear more accurate than those involving HNO_2, showing consistent ΔH values (−336 and −356 kJ · mol^{-1} for N_2O_3 and N_2O_4, respectively) under various conditions (temperature scan rate, N_2O_3/N_2O_4 stoichiometry…). From our calculated kinetic parameters, the rate constants extrapolated at 25°C lie around $k_{N_2O_3} \approx 10^8\ s^{-1}$ for N_2O_3, and $k_{N_2O_4} \approx 1.7\ s^{-1}$ for N_2O_4. However, such values do not take in account the quite probably different vapour pressures of N_2O_3 and N_2O_4, under the respective experimental conditions (different temperatures).

Discussion. Measured kinetic parameters and extrapolated rate constants at 25°C are quite consistent with literature reports on the reactivity of such nitrosating species in organic media.[14] However several questions arise from these experiments. Firstly, there is an important difference in the measured ΔH values which depend on the nitrosating agent, while similar values would have been expected. Much lower ΔH values with N_2O_3 (−336 kJ · mol^{-1}) and N_2O_4 (−356 kJ · mol^{-1}) than with $NaNO_2$ + TFA (−230 kJ · mol^{-1}) suggest the presence of additional exothermic processes in the former cases, for instance the hydrolysis of either N_2O_3 or N_2O_4 with water released by Val-NCA formation.

Also, the high values of activation energies ($E_A \approx$ 100–200 kJ · mol^{-1}, Tables 2–3) for these fast processes, primarily suggest these reactions to be dominated by entropic effects. Actually these reactions may be more complex than first-order, what might also explain the spectacular E_A increase in the nitrosation by {$NaNO_2$ + TFA} by increasing TFA/nitrite ratio (Table 2). Such E_A increase is probably related to important qualitative (mechanistic) changes. In all cases this means that the 1st-order kinetic model used probably provides quite inaccurate kinetic parameters E_A and A. Parallelly, such high E_A values may also be due to insufficient heat exchange between the reacting material and its environment, considering the high exothermicity of the process. In this respect, DSC monitoring at rate of 8°C min^{-1} which should minimise such effects (compared to those at 5°C min^{-1}), indeed results in smaller E_A values, cf. supporting information.

Further kinetic analysis by more sophisticated models is also complicated by the coexistence of several isomers of

Table 3. DSC data of reaction peak for nitrosation of C-Val (12.5 μmol) by excess N_2O_3 or N_2O_4 (stoichiometries in table): reaction enthalpy ΔH, DSC peak temperature T_m; calculated 1st-order kinetic parameters (activation energy E_A, pre-exponential factor A, extrapolated rate constant k at 25°C)

	N_2O_3				N_2O_4						
Reagent DSC rate (°C min^{-1})	**5**		**8**		**5**				**8**		
eq./C-Val	7.9	10.5	8.9	5.9	6.9	5.5	29.8	5.6	4.6	23.9	6.4
$-\Delta H$ (kJ.mol^{-1})	345.7	343.9	328.2	326.9	346.8	369.2	363.2	352.3	319.2*	342.2	365.2
T_m (°C)	−28.9		−28.7		−8.0				−4.2		
E_A (kJ.mol^{-1})	249.3 ± 0.2				102 ± 4						
A (s^{-1})	5.9 (±1.7) × 10^{51}				7.8 (±0.02) × 10^{18}						
k (s^{-1}, 25°C)	1.0 (±0.2) × 10^8				1.7 (±0.5)						

*These values were excluded in the calculation of averaged values.

DOI: 10.1002/poc

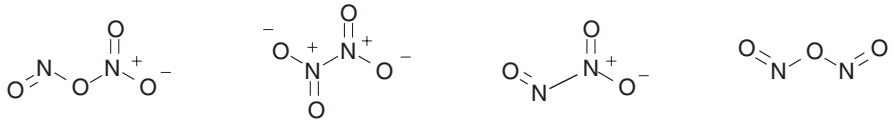

6 **7** **8** **9**

Scheme 3

both species N_2O_4 and N_2O_3[29] (Scheme 3), for which insufficient thermodynamic data are available, for example about interconversion equilibria. For instance, while the symmetrical isomer **6** is known as the most stable form of N_2O_4, its unstable, asymmetric isomer **7** (so-called nitrosyl nitrate) is often believed as the one effecting nitrosation.[14,29] Also, the asymmetric structure **8** is described as the most stable form of N_2O_3 in either gaseous or condensed phase, while nitrosation reactions may rather involve the unstable, symmetric isomer **9** preferentially formed by addition of NO + NO_2\cdot in condensed media,[29] but until now characterised only in solid argon matrix.[30–33]

The major influence of the O_2/NO ratio on the efficiency of solid C-Val nitrosation by the gaseous mixture NO + O_2, may therefore be interpreted in terms of changes in the availability of the involved nitrosating species, namely N_2O_3, N_2O_4 and HNO_2, the former being the most reactive.

Kinetic investigations of the solid-gas phase nitrosation

To circumvent the rapidity of the reaction at room temperature (usually less than 5–10 min), kinetic investigations were carried out at 0°C in the presence of excess NO_x, so that the pressure and stoichiometric composition of the equilibrated NO_x mixture should not significantly vary along the reaction.

We first investigated the evolution of the reaction extent. Solid C-Val (60–80 mesh powder) was reacted in a flat-bottom flask at 0°C under inert atmosphere (N_2). Gaseous NO was injected, then (at $t = 0$) O_2, so that O_2/NO = 1/4. At time t the reaction was quenched by a fast nitrogen flush, and the product distribution was determined by ^{1}H NMR in DMSO-d_6. Together with the expected Val-NCA, the reaction produced significant amounts of free valine, resulting from the hydrolysis of the NCA by water released during the reaction. The kinetics was monitored by repeating the reaction with quenching at various times. Results reported in Figure 3 show the process to be somewhat complex: we first observe an 1–2-min latency time (**A**), followed by a strong acceleration (**B**) for a few minutes, then a slower, linear evolution (**C**), until ca. 95% conversion is reached. Complete conversion was achieved within 20 min, where ca. 15% of NCA was hydrolysed into free valine. Noteworthy that the observed latency-acceleration sequence closely resembles a parabolic or exponential growth (cf. discussion section *infra*: Latency and acceleration steps).

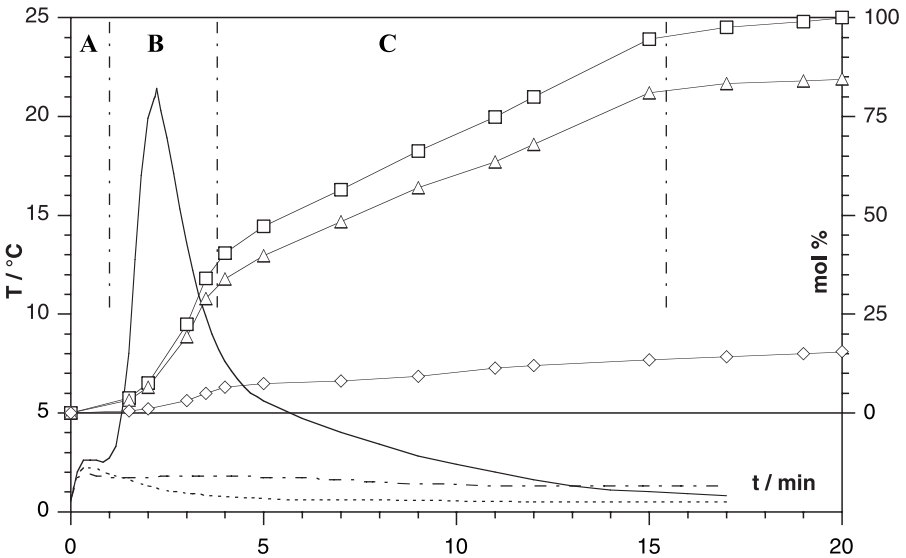

Figure 3. Nitrosation of C-Val in the dry phase at 0°C by 5 eq. NO + 1.25 eq. O_2 (O_2/NO = 0.25). Time evolution of conversion (squares) and products: Val-NCA (triangles), Val (diamonds) (measured by ^{1}H NMR); experimental points are connected visually for an easy reading. Curves: time evolution of temperature: of the gaseous phase (dash-dot line), of a blank experiment without C-Val (dotted line), of the solid substrate (continuous line) deposited onto the thermometer probe. Time domains *A*, *B*, *C* refer to latency, acceleration and zero-order kinetic steps, respectively (see text)

DOI: 10.1002/poc

This important increase in reaction rate, as well as the exothermicity of the overall process (occurring in a heterogeneous system), led to assume that the temperature of the condensed phase may be neither constant nor homogeneous, and to carry out calorimetric investigations. The use of microcalorimetric techniques was unsuccessful however: in the available set-up it was impossible to inject sufficient amounts of NO_x reagent (diluted in an N_2 stream) for any reaction to be observable. Alternately, we carried out rougher calorimetric investigations in the same glassware setup as above, by the use of the metallic probe of a conventional electronic thermometer (results on Figure 3). No significant temperature changes were recorded in the gas phase, except a small exotherm during the first 30 s, corresponding to NO autoxidation with O_2 since it was also present in a blank experiment without C-Val (cf. discussion *infra*). To monitor the temperature changes in the solid phase, a small amount of C-Val was recrystallised directly onto the thermometer probe then placed inside the set-up instead of being spread in the flask. In the typical temperature evolution profile (also shown on Figure 3), we observe first a small exotherm during the first 30 s (also observed when monitoring the temperature of the gas phase or in a blank experiment without C-Val), then a second, intense exotherm coincident with the acceleration step (**B**), followed by a pseudo-exponential decay coincident with the zero-order step (**C**).

Monitoring of either or both reaction extent or temperature was used to investigate various reaction parameters. Although our calorimetric technique did not allow to control the specific surface of the solid material, it appeared useful for investigating the reaction kinetics, in a more expedient way than quench/NMR techniques, thus allowing several complementary parameters to be investigated.

Effect of the specific surface of solid C-Val. The reaction was carried out on solid C-Val of various granulometries, obtained from sieving a single batch of recrystallised, then ground C-Val. Three fractions were obtained: 40–50 mesh ($\langle G\rangle = 358\ \mu m$, $S_{sp} = 136\ cm^2 \cdot g^{-1}$), 60–80 mesh (major: $\langle G\rangle = 211\ \mu m$, $S_{sp} = 231\ cm^2 \cdot g^{-1}$) and 180–400 mesh ($\langle G\rangle = 60\ \mu m$, $S_{sp} = 810\ cm^2 \cdot g^{-1}$). Specific surfaces S_{sp} are evaluated after solid C-Val density and average grain size. Using these three C-Val granulometries with the same O_2/NO stoichiometric ratio of 0.25, we observed very similar kinetic curves, all exhibiting the latency/acceleration/zero-order sequence. The curves appear almost superimposable after an overall streching/shrinking along the time axis. While the kinetic curves observed with the medium granulometry ($\langle G\rangle = 211\ \mu m$), or with the thickest granulometry ($\langle G\rangle = 358\ \mu m$) are almost identical as that obtained on the whole batch of ground C-Val, using the finest granulometry ($\langle G\rangle = 60\ \mu m$) results into a significantly accelerated process (Figure 4). This effect of solid specific surface was not investigated by calorimetric experiments where this parameter was not easily tunable.

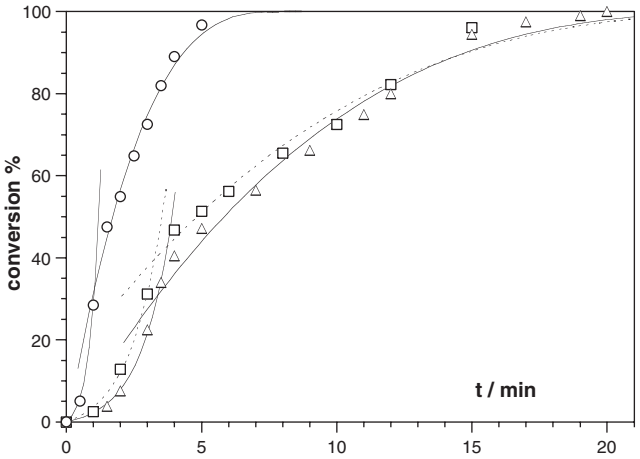

Figure 4. Effect of average C-Val granulometry $\langle G\rangle$ (circles: 60 μm, triangles: 211 μm, squares: 358 μm) on nitrosation of solid C-Val (0.125 mmol) by 5 eq. of NO and 1.25 eq. of O_2 (O_2/NO = 0.25). Curves (dotted lines: $\langle G\rangle = 358\ \mu m$): exponential growth (Eqn 9) and zero-order (with SUC model: Eqn 12) kinetic fits

Effect of NO/O_2 stoichiometric ratio. Symmetrically, the effect of NO_x mixture stoichiometry was also investigated on the 60–80-mesh ($\langle G\rangle = 211\ \mu m$) fraction. Kinetic results are shown in Figure 5. Again, we observed similar kinetic profiles, exhibiting the latency/acceleration/zero-order sequence, with a streching/shrinking along the time axis depending on the O_2/NO ratio: the highest O_2/NO, the fastest the kinetics is. Temperature-monitoring experiments provided similar results (Figure 6): an

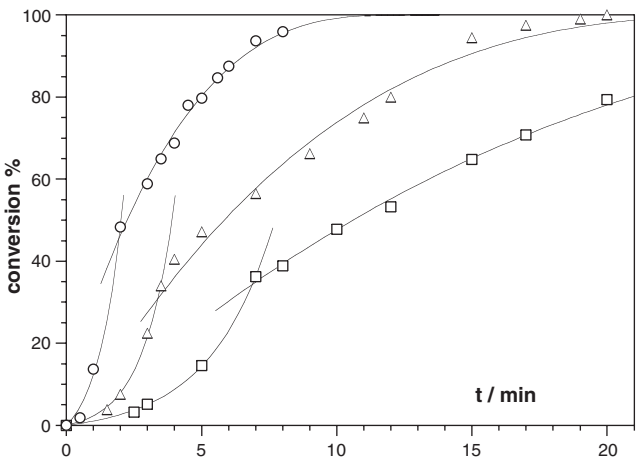

Figure 5. Effect of stoichiometric O_2/NO ratio (squares: 0.15, triangles: 0.25, circles: 0.40) on the kinetics of nitrosation of solid C-Val (0.125 mmol with average granulometry 211 μm) by 5 eq. of NO and either 0.75 (squares), 1.25 (triangles) or 2 eq. (circles) of O_2. Curves: exponential growth (Eqn 9) and zero-order (with SUC model: Eqn 12) kinetic fits

DOI: 10.1002/poc

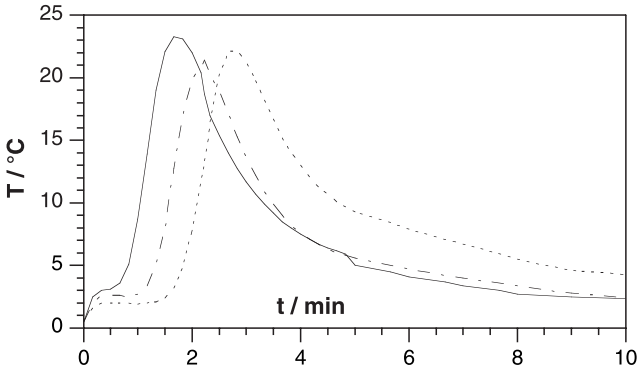

Figure 6. Effect of NO_x stoichiometry on nitrosation of solid C-Val at 0°C by 5 eq. NO + various amounts of O_2. Temperature of the solid (deposited onto the thermometer probe) as a function of time, under various O_2/NO ratios: 0.15 (dotted line), 0.25 (dash-dot line), 0.40 (solid line)

increase in the oxygen stoichiometry decreased the latency delay (from 1.5 min with O_2/NO = 0.15 to 40 s with O_2/NO = 0.4), meanwhile the main exotherm appeared sharper. This is consistent with different nitrosating ability along NO_x speciation as observed above, but it may also be correlated to faster/slower acidification of the medium (see Discussion below).

Effect of the NO/O_2 injection sequence. We investigated the possible coupling of NO autoxidation with O_2 (NO) with the nitrosation reaction, by varying the O_2/NO injection protocol. When NO and O_2 were injected sequentially over C-Val, we observed almost no difference (within experimental error) whether NO or O_2 was injected the first. When NO and O_2 were mixed prior to contact with C-Val, the first, small exotherm disappeared – thus confirming it is due to NO autoxidation – and the main exotherm (nitrosation) was both delayed (3.8 min vs. 2.3–2.5 min) and lowered. In all cases however, the conversion was complete after 1 h reaction. The boosting of the nitrosation step by the NO + O_2 autoxidation step may be due to either the exothermicity of the latter, or to the direct contact of C-Val with reactive NO_x intermediates (e.g. N_2O_3), possibly enhanced by the fact that NO + O_2 autoxidation may occur between adsorbed species.

Nevertheless in further experiments we adopted the NO-then-O_2 sequence (always used unless otherwise specified), for all NO + O_2 reactions with CAA, which provided both the easiest procedure, the most efficient reactivity, and the best reproducibility (e.g. against moisture effects, cf. *infra*).

Effects of moisture and amino acid hydrophobicity. The presence of moisture from the beginning of the reaction also accelerates the reaction. When the reaction is carried out under strictly dry conditions (carefully-dried vessel and reagents), both substantially increased latency time and weaker exotherm are observed compared to the reaction carried out without avoiding moisture (e.g. insufficient precautions taken by rainy weather). Conversely, the addition of a droplet (1–2 μl) of water into the set-up prior to O_2 injection results in an earlier, sharper exotherm. The same effect was observed (same changes in thermogramms) when using a premixed NO_x reagent, however with poorer reproducibility except under strictly dry conditions (e.g. NO—O_2 transfer under nitrogen counterflow). Such poor reproducibility is probably due to the high hygroscopicity of the NO_x mixture.

Alternately, a similar moisture effect was observed on thermogramms (both latency delay and main exotherm shape) when nitrosating various CAA such as C-Ala, C-Phe, C-Tyr by 5 eq. NO + 0.75 eq. O_2 under dry conditions: the observed relative reactivity of these CAA roughly followed the hydrophilicity order of their side-chains: C-Tyr ≈ C-Ala > C-Val > C-Phe. While the final conversion was complete after 1 h for C-Val and C-Ala, it was only 65% for C-Phe and ca. 51% for C-Tyr. Upon nitrosation of C-Tyr, a yellow-orange mixture was formed, possibly due to further nitrosation of the aromatic ring (prone to electrophilic substitutions because of the phenol group). Increasing the oxygen/NO ratio up to 0.40 in this case did not result in significant increase in conversion. Most likely, hydrophilicity (resp. hydrophobicity) of the side-chain of the amino acid contributes to retain (resp. repell) water evolved from NCA formation, thus having the same influence on the reaction kinetics as above.

Discussion: kinetic analysis

The behaviour of the system appears more complex here (Figures 4 and 5) than previously observed kinetics under fluid-bed conditions.[13] In such heterogeneous environment, the only convenient kinetic variable is the reaction extent ξ of the overall nitrosation reaction.

Latency and acceleration steps. In all experiments, the latency time **A** is roughly proportional to the acceleration time **B**, both steps being then possibly parts of a parabolic-shaped kinetic curve. Indeed steps (**A**–**B**) together can be accurately fitted with a function of type:

$$\xi = (k_0/k_1) \times (\exp(k_1 \cdot t) - 1) \quad (9)$$

which is a solution of the differential equation:

$$d\xi/dt = k_0 + k_1 \cdot \xi \quad (10)$$

with ξ being the reaction extent and k_0 the apparent rate constant at the beginning of the reaction (0°C). Meanwhile there is no evidence of any true latency delay before the parabolic growth (kinetic fits are not improved by replacing t by t–t_0 in Eqn 9). Both rate constants k_0 and k_1 globally increase with either the O_2/NO ratio or the specific surface S_{sp} of solid C-Val, however without any precise linear relationship.

DOI: 10.1002/poc

Equation 9 is a simple model for the kinetics of either an autocatalytic reaction occurring at constant temperature (k_1 then being the autocatalytic rate constant), or of an exothermic, zero-order reaction occurring in an adiabatic system, the latter in the approximations of both invariant heat capacity along the reaction and linear dependence of the rate constant k with temperature (e.g. a linear approximation of the Arrhenius law over a small temperature range).

Both the reaction exothermicity and the substantial temperature increase observed (Figs 3 and 6), strongly argue in favour of the second hypothesis, namely thermal self-acceleration. This would originate from quite slow heat diffusion throughout the solid C-Val or towards the (thermostated) walls of the vessel, compared to the nitrosation rate, surprisingly even for the slowest kinetics, for example with $O_2/NO = 0.15$, where Eqn 9 still accurately fits experimental data. Thermal self-acceleration has already been proposed to account for unaccountably high activation energies evaluated through DSC monitoring (cf. previous section).

A combination of both phenomena (thermal self-acceleration and autocatalysis) is also possible. It is worthy to note that, when water is present at the beginning of the reaction, its rate substantially increases over all steps; since the reaction itself releases water (together with NCA), this should logically act as an autocatalyst. Such autocatalysis may be chiefly physical however, through the formation of a liquid phase and dissolvation of solid reactants, thus increasing their molecular mobility.

Zero-order kinetics. The linear evolution sequence **C** (ca. 40–50% to ca. 90% conversion, assumed to occur at constant temperature) fits very well a zero-order kinetics, of rate k_{zero} (Table 4). To better account for the reaction in a powdered solid, we fitted our data with a shrinking unreacted core (SUC) model commonly used in solid-phase chemistry, which hypothesises the (zero-order) reaction to start at the surface of the material, then to propagate towards the core of the material, without diffusion of the reactants into the unreacted solid. With a simplified model assuming the powder to be made of identical, spherical particles, the kinetic law writes as:

$$d\xi/dt = k_{SUC} \times (1 - \xi)^{2/3} \tag{11}$$

which integrates as

$$\xi = 1 - (1 - k_{SUC} \times (t - t_0)/3)^3 \tag{12}$$

where k_{SUC} is the (particle-size dependent) rate constant and t_0 is the time at which the reaction is complete ($\xi = 1$). This model fits our data from 40–50% to 100% conversion (Table 4) with an accuracy similar to the linear fits of the 50–85% conversion range. Both k_{SUC} or k_{zero} rate constants increase with either the O_2/NO ratio or the specific surface S_{sp} of solid C-Val, however without precise linear relation.

The break in kinetic curves. We hold no definite explanation yet for the sudden break between self-accelerated kinetics (parabolic growth) and zero-order kinetics, systematically occurring at 40–50% conversion and coincident with the end of the exothermic peak on thermogramms, and which obviously denotes a significant change in the reaction process. As a first hypothesis (consistent with the rate increase with specific surface), if the self-accelerated step corresponds to the reaction of CAA with previously adsorbed NO_x species, then the break corresponds to either exhaustion of these adsorbed species, or to their desorption because of the temperature increase. Then the rate-limiting process in the subsequent zero-order step would be the slow adsorption of NO_x species.

Another, more plausible hypothesis is that this break would be the transition between a two-phase (solid-gas) and three-phase (solid-liquid-gas) system during the reaction, due to the accumulation of both water and nitric acid generated by the reaction. The formation of such a liquid phase may have several consequences, both physical an chemical:

- The formation of such a continuous liquid film between the (finely divided) solid C-Val substrate and the wall of the vessel (thermostated to 0°C) should ensure a

Table 4. Kinetic fits for solid C-Val nitrosation at 0°C by gaseous NO_x under various reaction conditions. Parameters of various (least square) fitting equations: Eqn 9 for exponential-growth sequence, $\xi = \xi_0 + k_{zero} \times t$ for zero-order fit, Eqn 12 for zero-order with SUC model

	Reaction parameters			Exponential growth fit			Zero-order fit		SUC fit	
O_2/NO	$p_{N_2O_4}$* (10^{-3} atm)	$\langle G \rangle$ (μm)	S_{sp} ($cm^2 \cdot g^{-1}$)	k_1 (min^{-1})	k_0 (min^{-1})	R^2	k_{zero} (min^{-1})	R^2	k_{SUC} (min^{-1})	R^2
0.15	12.1	211	231	0.425	0.00829	0.9997	0.034	0.9967	0.061	0.9954
0.25	23.3	358	136	0.824	0.0238	0.9968	0.044	0.9989	0.099	0.9722
0.25	23.3	211	231	0.885	0.0144	0.9981	0.047	0.9997	0.11	0.9789
0.25	23.3	60	810	3.09	0.0419	1.0000	0.17	0.9983	0.38	0.9862
0.4	41.6	211	231	1.08	0.0678	0.9938	0.099	0.9969	0.23	0.9906

*Calculated at 0 °C and constant volume in an equilibrated mixture of 0.14 atm of NO with appropriate O_2 pressure, cf. Supporting Information.

DOI: 10.1002/poc

more efficient heat transfer, with sudden chilling of the substrate, significantly lowering the reaction rate and breaking the self-accelerated kinetics.

- Retarded water evaporation, occurring only once a threshold temperature is attained in the substrate: such heat dissipation may contribute to lower the temperature of the substrate, thus decreasing the reaction apparent rate. This effect is probably weak however: the vaporisation heat of water (ca. $10\,kcal \cdot mol^{-1}$) is indeed significantly lower than the nitrosation exothermicity (ca. $80\,kcal \cdot mol^{-1}$, *vide supra*).
- A change in the nature of the nitrosating species (*vide supra*): while in the solid-gas process the reaction is probably mediated by reactive covalent species (N_2O_3, N_2O_4), once a liquid phase is formed the nitrosating species might be ions, such as NO^+ (from dissociation of either N_2O_3 or N_2O_4) or $H_2NO_2^+$ (from protonation of HNO_2), due to the acidity of this liquid phase also resulting from partial hydrolysis of N_2O_3 and N_2O_4 into HNO_2 and HNO_3, respectively. We observed (cf. above) the intrinsic reactivity of $H_2NO_2^+/NO^+$ to be lower than that of either N_2O_3 or N_2O_4.

Acidity and N_2O_4. Nevertheless this change in nitrosating intermediates is probably not the main cause of the kinetic break. Indeed, we observed sharper exotherms and increased rates of both self-accelerated and zero-order steps when the reaction was carried out with either added water at the reaction beginning, or with increased O_2/NO ratios (Figures 5 and 6), while both factors contribute to the release of more nitric acid, therefore to the formation of increased NO^+ amounts. This acidification of the medium is probably the cause of the apparent catalytic effect of N_2O_4: when varying the O_2/NO ratio, increments in rate constants (Table 4) almost linearly follow the equilibrium partial pressure of N_2O_4 (itself increasing with the O_2/NO ratio). Further investigations would be necessary to definitely conclude on this point.

CONCLUSIONS

We have highlighted the major influence of the O_2/NO ratio on the efficiency of solid C-Val nitrosation by gaseous $NO + O_2$ mixtures, probably due to the changing availability of involved nitrosating species, namely N_2O_3, N_2O_4 and HNO_2 (the latter formed in contact with water). Thermoanalytical investigation of the reaction effected by either of the above species allowed to evaluate and compare their rate constants, showing that N_2O_3 is by far the most reactive under our conditions. To the best of our knowledge, this is the first report of such kinetic results concerning the nitrosation of CAA in the solid phase. Meanwhile, we also report the measurement of the latent heat of fusion of N_2O_3 ($2.74\,kJ \cdot mol^{-1}$) for the first time. Comparison of the $\{NO + O_2\}$ nitrosating systems to {sodium nitrite + TFA} for NCA synthesis shows the former to be more efficient in terms of either reagent stoichiometric demand, reaction rate, or further tractability of the crude product.

Kinetic investigation of solid-phase nitrosation of CAA by gaseous NO_x is a challenging problem due to the number of both physical and chemical elementary steps involved, with insufficient knowledge on many of them. Moreover such kinetic investigation of solid-gas reactions is not frequent in fine organic chemistry. Our investigations on solid *N*-carbamoyl valine nitrosation by gaseous NO_x revealed two distinct kinetics in the course of the reaction: first an unexpected auto-accelerating step with exponential growth, followed by a (pseudo)zero-order step beyond ca. 40–50% conversion. While the rationalisation of each step is possible separately if considering temperature increase due to exothermicity, possible (auto)catalytic effects related to water formation, or pseudo-zero-order kinetics in a SUC model, several hypotheses/explanations remain possible concerning the neat transition between these two kinetic behaviours, which may involve both physical (e.g. formation of a liquid phase) and chemical (depletion of adsorbed reactive species, or change in reaction intermediates) factors.

Beyond the interest of this reaction in the field of molecular origins of life as a possible prebiotic pathway from amino acids toward peptides on the primitive Earth,[13,34] further investigation is in progress to improve the efficiency and selectivity of this NCA synthesis in a preparative scope, also examining alternative nitrosating systems, such as nitrosyl halides.

EXPERIMENTAL SECTION

Caution: hazardous compounds

Nitric oxide is skin- and mucous-irritant. Nitrosoureas are potent carcinogens. All operations involving the handling of these compounds or their solutions were carried out wearing gloves in a fume hood. Effluents were destroyed by treatment with concentrated aqueous sodium hydroxide.

Materials and methods

Methanol was obtained from Baeckeroot (France). Alanine, valine, phenylalanine, tyrosine were obtained from Aldrich. Potassium cyanate was obtained from Prolabo. Hydrochloric acid (36%) was obtained from Carlo Erba (France). Nitric oxide and oxygen were obtained from L'Air Liquide (France).

Potassium cyanate was washed with methanol then dried *in vacuo* prior to use in order to remove ammonia

DOI: 10.1002/poc

traces. All other reagents and solvents were used as received. Gaseous NO and O_2 were handled in separate glass syringes at room temperature and under atmospheric pressure.

Physical measurements

^{1}H-NMR spectra were recorded on a Bruker AC200 or AC250 spectrometer (200 or 250 MHz, respectively) in DMSO-d_6 solution.

Capillary electrophoretic (CE) separations were performed using an automated CE apparatus (Beckman P/ACE MDQ, Fullerton, CA, USA) with a negative polarity on the inlet side of the capillary. Fused-silica capillary – (Cil Cluzeau) 50 μm i.d. × 30 cm (20 cm to the detector) – was initially conditioned with sodium hydroxide (0.1 M for 15 min under a pressure of 20 psi). Prior to analysis, the capillary was washed with 0.1 M NaOH (20 psi for 1 min), MΩ water (20 psi for 0.5 min) and background electrolyte (20 psi for 10 s). The capillary was thermostated at 25°C. Samples were introduced hydrodynamically by the application of a positive pressure of 0.3 psi for 10 s. Nitrate and nitrite were monitored by UV absorption at 214 nm. The experiments were carried out applying a constant voltage of −10 kV. The background electrolyte was a 10 mM (pH 8.5) borate buffer containing 150 mM of sodium chloride.

DSC analyses were performed using a Mettler-Toledo DSC–30 apparatus coupled with a TA4000 processor and monitored using the GraphWare TA72 software, using sealable, stainless-steel crucibles (120 μl, 20 bar) obtained from Mettler-Toledo.

X-ray diffraction analysis of C-Val was carried out on a 4-circle CAD4 diffractometer with $\lambda = \mathrm{Mo}K\alpha$. Although the molecular structure was unambiguously established, standard deviations on bond lengths and angles were too large (due to poor quality of C-Val single crystals) to be worthy of separate publication (cf. Supporting Information). Powdered solid C-Val density was measured using a Micromeritics AccuPyc 1330 pycnometer.

Microcalorimetry experiments were carried out using a Microscal Ltd Flow Microcalorimeter (FMC) system including a thermal conductivity detector (130°C), a Bronkhorst High-Tech flowmeter and a Kipp & Zonen integrator. Temperature monitoring of C-Val reaction was realised by means of a Checktemp 1 electronic thermometer (metallic thermal probe).

N-Carbamoylamino acids

N-carbamoylvaline C-Val, *N*-carbamoylphenylalanine C-Phe and *N*-carbamoylalanine C-Ala were prepared according to our previously published procedure.[15] Solid C-Val of selected granulometry was obtained by grinding pure C-Val then sieving through 80–40, 246–175 and 400–315 μm sieve pairs. X-ray analysis of C-Val were performed on a C-Val single crystal prepared by slow recrystallisation from water.

N-carbamoyltyrosine C-Tyr was prepared using the procedure described for C-Val, using 5 g (27.6 mmol) tyrosine and 4.48 g (55.2 mmol) potassium cyanate in 50 ml water at 50°C, pH 7.5 for 15 h. The reaction mixture was concentrated in vacuo at 30°C to half-volume then acidified to pH 2. After recrystallisation from boiling water, 4.58 g (74%) pure material was obtained. δ_H 2.80 (2H, ABX syst., H_β, $J_{\alpha\beta} = 5.5$ Hz, $J_{\alpha\cdot\beta} = 7.5$ Hz, $J_{\beta\beta'} = 14$ Hz); 5.65 (2H, s, —NH_2), 4.26 (1H, ABX syst., H_α, $J_{\alpha\cdot\beta} = 5.5$ Hz, $J_{\alpha\beta} = J_{\alpha-NH} = 8.0$ Hz), 6.08 (1H, d, —NH—, $J_{\alpha-NH} = 8.0$ Hz), 6.75 (2H, d, H_1), 6.98 (2H, d, H_2), 9.23 (1H, s, —OH), 12.56 (1H, s, —COOH). δ_C 37.67 (C_β), 54.78 (C_α), 115.80 (C1), 128.96 (—C_{Ar}—CH_2—), 130.97 (C_2), 156.76 (—C_{Ar}—OH), 158.95 (—NH—CO—NH_2), 174.90 (COOH).

Nitrosation of C-Val by $NaNO_2$ + TFA in acetonitrile suspension

In a 100-ml glass flask fitted with a magnetic stirrer were introduced 100 mg (625 μmol) C-Val, appropriate amount of sodium nitrite and acetonitrile (50–*y* ml, *y* being related to the amount of TFA to be added). The flask was closed with a silicon rubber cap, then flushed with either helium or nitrogen for 30 min, then *y* ml of a 0.375 M solution of TFA in acetonitrile was injected into the vessel by means of a glass syringe. Either of the following procedures was then applied:

a) After stirring for 5 min at room temperature, the reaction was quenched by injection of an excess 1 N aqueous sodium hydroxide into the vessel. After *in vacuo* evaporation of the solvents, the residue was dissolved in 50 ml of HPLC eluent (water/acetonitrile: 90/10 v/v), and analysed by HPLC for remaining C-Val titration.
b) After reaction completion (30–120 min), the setup was flushed by nitrogen for 10 min then the solvent was removed *in vacuo*. The residue was then dissolved in DMSO-d_6 for NMR analysis.

Nitrosation of C-Val by NO + O_2 in acetonitrile suspension

A 100-ml glass flask fitted with a magnetic stirrer and containing 100 mg (625 μmol) of C-Val in 50 ml acetonitrile was closed with a silicon rubber cap and flushed by nitrogen for 20 min (by means of steel needles through the silicon cap). 14, 28 or 42 ml (0.625, 1.25 or 1.88 mmol, respectively) of gaseous NO was then injected into the setup, followed by the appropriate amount of O_2 by means of glass syringes. After stirring

DOI: 10.1002/poc

for 30 min at room temperature, the setup was flushed by nitrogen for 10 min, and the solvent was removed *in vacuo* (rotary evaporator). Either of the following procedures was then applied:

a) The residue was dissolved in DMSO-d_6 for NMR analysis.
b) The residue was dissolved in 50 ml of HPLC eluent (water/acetonitrile: 90/10 v/v), and analysed by HPLC for remaining C-Val titration.

Nitrosation of C-Val (solid-gas phase)

A 29-ml, flat-bottom glass reactor containing 30 mg (187.5 μmol) of C-Val (ground to mesh-size 246–175 μm) was closed with a silicon rubber septum and flushed by nitrogen for 10 min (by means of steel needles through the silicon cap). 4.2 ml (187.5 μmol, 1 eq.) gaseous NO was then injected into the setup, followed by the appropriate amount of O_2 (0.2 to 6.0 ml) by means of glass syringes. After 30 min stirring at room temperature, either of the following procedures was applied:

a) The setup was flushed by nitrogen for 10 min, then the residue was dissolved in DMSO-d_6 for NMR analysis.
b) 5 ml aqueous NaOH 0.2 N was injected into the reaction mixture, which was then stirred for 1 h at rt. 1 ml aqueous KBr ($c = 8.412 \times 10^{-3}$ mol · L^{-1}) was added to the mixture which was then diluted to 100 ml in water. An 1 ml aliquot of this solution was submitted to CE analysis for nitrite and nitrate quantification. Migration times (min) under the used conditions: 2.45 (Br^-: reference), 2.85 (NO_2^-), 3.05 (NO_3^-). Extinction coefficients were previously calibrated using standard solutions.

Blank experiments

Estimation of N_2O_3/N_2O_4 hydrolysis. The same setup as above was flushed with nitrogen for 10 min, then appropriate amounts of NO and O_2 were injected by means of glass syringes. 2 μl of either saturated aqueous NaCl or 50% aqueous HNO_3 were then injected into the setup. After 10 min reaction, 5 ml of 0.2 N aqueous NaOH were injected into the setup, while this was quickly flushed with nitrogen for a few seconds. The resulting aqueous mixture was stirred for 1 h then worked up as above for CE analysis.

Evaluation of alkaline dismutation of NO. The above 29-ml reactor containing 30 mg (187.5 μmol) of C-Val (ground to mesh-size 246–175 μm) and appropriate amounts of $NaNO_2$ and $NaNO_3$, was closed with a silicon rubber septum and flushed by nitrogen for 10 min at room temperature, prior to the injection of the appropriate amount of NO. The system was immediately quenched by injection of 5 ml of 0.2 N NaOH then worked up as above for CE analysis.

DSC monitoring of C-Val nitrosation

To avoid any premature reaction, all reagents were frozen with liquid-nitrogen prior to any contact with each other until DSC experiments.

Nitrosation by HNO_2. Finely powdered C-Val (2 mg, 12.5 μmol) and $NaNO_2$ were introduced into the DSC crucible, which was then frozen (liq. N_2) prior to introduction of frozen TFA. The crucible was sealed then stored in liquid nitrogen until being placed into the (pre-frozen) DSC cell. Temperature scanning: −100°C to +30°C at rate 5 or 8°C min^{-1}.

Nitrosation by N_2O_4. Solid (liq. N_2-frozen) N_2O_4 was introduced into the cold DSC crucible, which was then immediately frozen in liquid nitrogen. A small, open PTFE cup (hand-made from PTFE 1/8″ tubing) containing 2 mg (12.5 μmol) of finely powdered C-Val, was then placed into the crucible (on top of solid N_2O_4). The sealed crucible was stored in liquid nitrogen until being placed into the (pre-frozen) DSC cell. Temperature scanning: −80°C to +50°C at either 5 or 8°C min^{-1}.

Nitrosation by N_2O_3. Same procedure as above, using solid (liq. N_2-frozen) N_2O_3 instead of N_2O_4. Temperature scanning: −150°C to +10°C at either 5 or 8°C min^{-1}.

Preparation of N_2O_3:[27] 15 ml of 70% aqueous nitric acid was added dropwise to 8 g, (40.4 mmol) of dry As_2O_3 placed under inert atmosphere in a magnetically stirred, chilled (ice-bath), closed flask. The evolving dark-brown-reddish gas was directly condensed at −10°C in a separate flask as a dark-blue liquid, where it was stored as a liquid under saturating NO atmosphere.

Solid-Phase nitrosation of C-Val: kinetic experiments

In a 100–ml glass-reactor was introduced 20 mg (125 μmol) of C-Val of appropriate granulometry. The reactor closed with a silicon-rubber septum was flushed by nitrogen (by means of steel needles through the septum) for 10 min at room temperature, then for 15 min at 0°C (ice-water bath). After a few minutes standing, 14 ml (625 μmol, 5 eq.) NO then a selected amount of O_2: 2.1 ml (93.8 μmol, 0.75 eq.), 3.5 ml (156 μmol, 1.25 eq.) or 5.6 ml (250 μmol, 2 eq.) were rapidly injected into the reactor by means of glass syringes. After a given time t (O_2 injection being done as $t = 0$) the reaction was quenched by a fast nitrogen flush and the setup was warmed to rt, then the crude product was immediately dissolved in DMSO-d_6 and analysed by ^{1}H NMR.

DOI: 10.1002/poc

Nitrosation of C-Val with temperature monitoring

The same setup as above was used, with the probe of an electronic thermometer fitted through the silicon-rubber cap. 25 mg (156 μmol) C-Val was deposited onto the metallic thermal probe by repeated recrystallisation from a saturated methanol solution (2–3 recrystallisation layers were usually necessary; the amount of C-Val deposited was checked by weighting the probe before and after deposition). The probe covered by C-Val was dried in vacuo at 30°C prior to introduction into the reactor. The setup was then thermostated to 0°C (crushed-ice bath) and flushed with nitrogen prior to injection of NO and O_2 (same amounts and protocol as above). The temperature was monitored every 5 or 10 s along the reaction (O_2 injection was taken as $t = 0$). At the end of the reaction (ca. 20 min), the setup was flushed with nitrogen and warmed up to rt, then the crude solid was immediately dissolved in DMSO-d_6 and analysed by ^{1}H NMR.

Reverse O_2-NO injection sequence. The same protocol as above was applied except O_2 was injected before NO. NO injection was taken as time $t = 0$.

Premixed-NO_x injection. The same protocol as above was applied; the mixing of O_2 and NO was realised immediately prior to injection into the nitrosation setup. 2.1 ml of O_2 was first loaded into the glass syringe, which was then connected to the NO delivery setup. A pressure slightly exceeding atm pressure was applied to load 14 ml NO, cheked on syringe graduations. The gas mixture was allowed to stand for ca. 30 s prior to injection into the nitrosation setup. When dry conditions were required, the whole O_2/NO handling process was carried out under nitrogen flush.

Nitrosation of C-Ala, C-Phe, C-Tyr with temperature monitoring

The same procedure as for C-Val was applied using either 21 mg (159 μmol) of C-Ala, 30 mg (144 μmol) of C-Phe, or 36 mg (161 μmol) of C-Phe (all crystallised onto the thermometer probe from saturated methanol solution) instead of C-Val. The NO-then-O_2 injection sequence was applied in all cases.

Supplementary Material

Supporting information is available in Wiley InterScience at http://www.interscience. wiley.com/jpages/0894-3230/suppmat/.

Acknowledgements

This work was financially supported by the CNRS, the French Ministry of Education and Research, and by Degussa AG (Germany). We are grateful to Dr Francis Carré from Chemistry Departmen, University of Montpellier 2 for X-ray diffraction measurements.

REFERENCES

1. Leuchs H. *Ber. Dtsch. Chem.* 1906; **39**: 857–861.
2. Farthing AC, Reynolds RJW. *Nature* 1950; **165**: 647.
3. Coleman D, Farthing AC. *J. Chem. Soc. Abstr.* 1951; 3218–3222.
4. Kricheldorf HR. *α-Aminoacid-N-Carboxy-Anhydrides and Related Heterocycles. Synthesis, Properties, Peptide Synthesis, Polymerisation*. Springer-Verlag: Berlin, 1987.
5. Wilder R, Mobashery S. *J. Org. Chem.* 1992; **57**: 2755–2756.
6. Taillades J, Beuzelin I, Garrel L, Tabacik V, Commeyras A. *Orig. Life Evol. Biosphere* 1998; **28**: 61–77.
7. Collet H, Bied C, Mion L, Taillades J, Commeyras A. *Tetrahedron Lett.* 1996; **37**: 9043–9046.
8. Meijide F, Vazquez Tato J, Casado J, Castro A, Mosquera M. *J. Chem. Soc., Perkin Trans. 2* 1987; 1759–1765.
9. Darbeau RW, Pease RS, Perez EV. *J. Org. Chem.* 2002; **67**: 2942–2947.
10. Baldwin JE. *J. Chem. Soc. Chem. Commun.* 1976; 734–736.
11. Baldwin JE, Cutting J, Dupont W, Kruse L, Silberman L, Thomas RC. *J. Chem. Soc. Chem. Commun.* 1976; 736–741.
12. Suzuki M, Yamazaki T, Ohta H, Shima K, Ohi K, Nishiyama S, Sugai T. *Synlett* 2000; 189–192.
13. Taillades J, Collet H, Garrel L, Beuzelin I, Boiteau L, Choukroun H, Commeyras A. *J. Mol. Evol.* 1999; **48**: 638–645.
14. Williams DLH. *Nitrosation*. Cambridge University Press: Cambridge, 1988.
15. Taillades J, Boiteau L, Beuzelin I, Lagrille O, Biron J-P, Vayaboury W, Vandenabeele-Trambouze O, Giani O, Commeyras A. *J. Chem. Soc., Perkin Trans. 2* 2001; 1247–1254.
16. Rice DE, Crawford GH. *J. Org. Chem.* 1963; **28**: 872–873.
17. Stedman G. *J. Chem. Soc. Abstr.* 1960; 1702–1709.
18. Casado J, Castro A, Lopez Quintela MA, Mosquera M, Rodriguez Prieto MF. *Monatsh. Chem.* 1983; **114**: 647–660.
19. Casado J, Castro A, Mosquera M, Rodriguez Prieto MF, Vazquez Tato J. *Monatsh. Chem.* 1984; **115**: 669–682.
20. Verhoek FH, Daniels F. *J. Am. Chem. Soc.* 1931; **53**: 1250–1263.
21. Beattie IR, Bell SW. *J. Chem. Soc.* 1957; 1681–1686.
22. Lide DR. *Handbook of Chemistry and Physics*, 81st edition. CRC Press: Boca Raton, FL, 2000.
23. Bravo C, Hervès P, Leis JR, Pena ME. *J. Chem. Soc., Perkin Trans. 2* 1991; 2091–2095.
24. Singer K, Vampley PA. *J. Chem. Soc.* 1956; 3971–3974.
25. Ridd JH. *Quart. Rev.* 1961; **15**: 418–441.
26. Kim JC, Cho IS, Choi SK. *J. Korean Chem. Soc.* 1991; **35**: 240–248.
27. Schenk PW. In *Handbook of Preparative Inorganic Chemistry*, Brauer G (ed.). Academic Press: New York, 1963.
28. In *Encyclopedie des gaz - L'air Liquide*. Elsevier: Amsterdam, 1976; 1065–1072.
29. Challis BC, Kyrtopoulos SA. *J. Chem. Soc., Perkin Trans. II* 1978; 1296–1302.
30. Hisatsune IC, Davlin JP, Wada Y. *J. Chem. Phys.* 1960; **33**: 714–719.
31. Varetti EL, Pimentel GC. *J. Chem. Phys.* 1971; **55**: 3813–3821.
32. Nour EM, Chen LH, Laane J. *J. Phys. Chem.* 1983; **87**: 1113–1120.
33. Wang X, Qin Q-Z. *Spectrochim. Acta A* 1998; **54**: 575–580.
34. Commeyras A, Collet H, Boiteau L, Taillades J, Vandenabeele-Trambouze O, Cottet H, Biron J-P, Plasson R, Mion L, Lagrille O, Martin H, Selsis F, Dobrijevic M. *Polym. Int.* 2002; **51**: 661–665.

DOI: 10.1002/poc